American College of
Neuropsychopharmacology

ARTICLE

Check for updates

In vivo brain endocannabinoid metabolism is related to hippocampus glutamate and structure – a multimodal imaging study with PET, 1H-MRS, and MRI

Jeremy J. Watts[1,2,3], Elisa Guma[4,5], Sofia Chavez[6,7,8], Rachel F. Tyndale [3,8], Ruth A. Ross[3], Sylvain Houle[6,7], Alan A. Wilson[6], Mallar Chakravarty[4,9,10], Pablo M. Rusjan [9,10] and Romina Mizrahi [9,10 ✉]

Dysregulation of hippocampus glutamatergic neurotransmission and reductions in hippocampal volume have been associated with psychiatric disorders. The endocannabinoid system modulates glutamate neurotransmission and brain development, including hippocampal remodeling. In humans, elevated levels of anandamide and lower activity of its catabolic enzyme fatty acid amide hydrolase (FAAH) are associated with schizophrenia diagnosis and psychotic symptom severity, respectively (*Neuropsychopharmacol*, 29(11), 2108–2114; *Biol. Psychiatry* 88 (9), 727–735). Although preclinical studies provide strong evidence linking anandamide and FAAH to hippocampus neurotransmission and structure, these relationships remain poorly understood in humans. We recruited young adults with and without psychotic disorders and measured FAAH activity, hippocampal glutamate and glutamine (Glx), and hippocampal volume using [11C]CURB positron emission tomography (PET), proton magnetic resonance spectroscopy (1H-MRS) and T1-weighted structural MRI, respectively. We hypothesized that higher FAAH activity would be associated with greater hippocampus Glx and lower hippocampus volume, and that these effects would differ in patients with psychotic disorders relative to healthy control participants. After attrition and quality control, a total of 37 participants (62% male) completed [11C]CURB PET and 1H-MRS of the left hippocampus, and 45 (69% male) completed [11C]CURB PET and hippocampal volumetry. Higher FAAH activity was associated with greater concentration of hippocampal Glx ($F_{1,36.36} = 9.17$, $p = 0.0045$; Cohen's $f = 0.30$, medium effect size) and smaller hippocampal volume ($F_{1,44.70} = 5.94$, $p = 0.019$, Cohen's $f = 0.26$, medium effect size). These effects did not differ between psychosis and healthy control groups (no group interaction). This multimodal imaging study provides the first in vivo evidence linking hippocampal Glx and hippocampus volume with endocannabinoid metabolism in the human brain.

INTRODUCTION

The hippocampus plays critical roles in cognition and emotion, and deviations from healthy structure and function are observed in psychotic disorders, including elevated glutamate, increased energy metabolism and reduced grey matter volume, with pathology beginning at CA1 and spreading outwards with disease progression [1]. Hippocampus neurotransmission and plasticity are regulated by the endocannabinoid system, which also contributes to hippocampus development [2–4] and neurogenesis [5, 6]. In addition to regulating neuronal excitability and presynaptic neurotransmitter release at most synapses in the brain [7, 8], the endocannabinoid system has roles in brain development, synaptic plasticity and neuronal survival [9].

The endocannabinoids anandamide and 2-AG act primarily through activation of cannabinoid CB1 receptors [10], although anandamide may also modulate hippocampus neurotransmission through TRPV1 receptors [11, 12]. Endocannabinoid system disturbances in schizophrenia include reduced in vivo CB1 receptor binding in the brain and elevated anandamide in blood and cerebrospinal fluid [13, 14]. In the brain, anandamide (but not 2-AG) content was reduced in post-mortem hippocampus of patients [15]. Anandamide tissue levels are governed primarily by its catabolic enzyme fatty acid amide hydrolase (FAAH; [16]). In vivo, brain FAAH activity was unaltered in psychosis patients [17], however lower brain FAAH activity was associated with greater positive psychotic symptom severity (delusions, hallucinations, suspiciousness, unusual thought content; [17]).

Preclinical studies have established contributions of FAAH in the development and maintenance of hippocampal neurons and synapses, neuroplasticity and hippocampus-mediated behaviors

---

[1]Research Centre, CHU Sainte-Justine, Montreal, QC, Canada. [2]Department of Psychiatry, Université de Montréal, Montreal, QC, Canada. [3]Department of Pharmacology & Toxicology, University of Toronto, Toronto, ON, Canada. [4]Computational Brain Anatomy (CoBrA) Laboratory, Cerebral Imaging Centre, Douglas Mental Health University Institute, Montreal, QC, Canada. [5]Developmental Neurogenomics Unit, Human Genetics Branch, National Institute of Mental Health, Bethesda, MD, USA. [6]Brain Health Imaging Centre, Centre for Addiction and Mental Health, Toronto, ON, Canada. [7]Department of Psychiatry, University of Toronto, Toronto, ON, Canada. [8]Campbell Family Mental Health Research Institute, Centre for Addiction and Mental Health, Toronto, ON, Canada. [9]Department of Psychiatry, McGill University, Montreal, QC, Canada. [10]Douglas Mental Health University Institute, Montreal, QC, Canada. ✉email: romina.mizrahi@mcgill.ca

[18–21] and modulation of hippocampal glutamate neurotransmission at the synaptic and neuronal population levels [18, 22]. In rodents, pharmacological inhibition or gene knockout of FAAH led to increased BDNF and hippocampus cell proliferation [23–25], supporting a plausible role of FAAH in hippocampus structure in the adult brain. Further, FAAH overexpression led to elevated excitatory and inhibitory neurotransmission [18], supporting a role of FAAH activity in hippocampus glutamate neurotransmission. In humans, the *FAAH* rs324420 (C385A) polymorphism affects the expression levels of FAAH, carriers of the variant A-allele exhibiting lower levels of FAAH protein [26]. Carriers of the FAAH A-allele have been reported to exhibit altered activity in several brain regions including the hippocampus, amygdala and ventromedial prefrontal cortex [27–29].

Whereas evidence from preclinical studies has established a role of the endocannabinoid system in hippocampal structure and neurotransmission (11, 20; and as described above) no study to date has explored this in living humans. Here, we measured brain FAAH activity, hippocampal glutamate metabolites (glutamate and glutamine, hereafter, Glx), and hippocampus volume in young adults with and without psychotic disorders using positron emission tomography (PET), proton magnetic resonance spectroscopy (^{1}H-MRS) and structural magnetic resonance imaging (MRI).

In animals, elevated FAAH activity is associated with increased excitatory neurotransmission [18] whereas reduced FAAH activity (or increases in anandamide) is associated with elevated hippocampus cell proliferation and BDNF [2, 23–25, 30, 31]. Therefore, in healthy control participants, we hypothesized that higher FAAH activity would be associated with higher hippocampus Glx and smaller hippocampus volume. In psychosis patients there is strong evidence for elevated hippocampus Glx and lower hippocampus volume [32, 33], therefore, we hypothesize that the associations of FAAH with Glx and hippocampus volume will differ in schizophrenia relative to observations in the healthy control group.

MATERIALS AND METHODS
Participants
Details regarding study participants for each analysis ([^{11}C]CURB and hippocampus Glx & [^{11}C]CURB and hippocampus volume), including neuroimaging quality control and *FAAH* rs324420 genotyping are provided in the results section and Supplementary Materials. Patients in the psychotic spectrum met criteria for a DSM-IV psychotic disorder (schizophrenia, schizophreniform disorder, delusional disorder, psychosis not otherwise specified) as determined by the structured clinical interview for DSM-IV (SCID) and confirmed by a trained psychiatrist (RM). Symptom severity was rated using the Positive and Negative Syndrome Scale (PANSS; [34]). Healthy control participants had no history of psychiatric illness including substance abuse or dependence (except nicotine or caffeine) as determined by the SCID and no history of psychotic disorders in first-degree relatives. Drug use history was assessed by a semi-structured interview and current use was tested using a urine drug screen. Participants were excluded if they were pregnant, breastfeeding, or had a medical illness or metal implants precluding MRI. Participant data reported in this publication partially overlap with previously published cohorts, including hippocampus ^{1}H-MRS [35], hippocampal volume [36], and [^{11}C]CURB λk3 [17].

This study was approved by the Research Ethics Board at the Centre for Addiction and Mental Health (CAMH). All participants provided written informed consent after receiving a description of all study procedures. All psychosis patients demonstrated capacity to provide informed consent as assessed by MacCAT [37].

Positron emission tomography
PET scans were performed using a 3D brain high resolution research tomograph (HRRT; CPS/Siemens, Knoxville, TN, USA), which measures radioactivity in 207 slices with an interslice distance of 1.22 mm. To reduce head movement, each participant was fitted with a custom thermoplastic mask used with a head-fixation system. A transmission scan using a single

photon point source, 137Cs ($t_{1/2} = 30.2$ years, $E\gamma = 662$ keV), was acquired to correct the emission data for the attenuation of the emission photons through the head and support. Following a transmission scan, an intravenous bolus of [^{11}C]CURB (357 ± 28 MBq) was infused over 1 min at a constant rate (Harvard Apparatus, Holliston, MA, USA) and dynamic PET data were acquired in for the next 60 min. Arterial samples were taken continuously for the first 22.5 min after [^{11}C]CURB injection with an automatic blood sampling system (Model PBS-101, Veenstra Instruments, The Netherlands). Manual samples were taken 3, 7, 12, 15, 20, 30, 45, and 60 min after injection. Radioactivity in whole blood and plasma (1500 g, 5 min) was counted using a Packard Cobra II or Wizard *470 γ-counter cross-calibrated with the PET system. Concentration of the parent radioligand and its metabolites was determined in each manual sample (except the one at 15 min). Blood-to-plasma radioactivity ratios were fitted using a biexponential function and parent plasma fraction using a Hill function. A metabolite-corrected arterial plasma input function was generated as previously described [38]. [^{11}C]CURB binding was quantified using the validated two-tissue-compartment model with irreversible binding (2-TCMi). The validated outcome measure for [^{11}C]CURB quantification is the composite parameter λk3, which is independent of blood flow, and is proportional to the amount of [^{11}C]CURB bound to FAAH. As [^{11}C]CURB binds to the active site of FAAH [39–41], [^{11}C]CURB λk3 should be proportional to the concentration of available FAAH active sites. Proton density (PD)-weighted brain MR images required for the delineation of each region of interest were obtained for each subject using a 3 T MR-750 scanner (General Electric Medical Systems). The creation of input functions from blood data as well as the extraction of time-activity curves for each region were performed using a validated and reproducible in-house imaging pipeline [42].

The *FAAH* rs324420 genotype was determined using DNA samples from blood and a Taqman SNP genotyping assay (probe: cat#C___1897306_10, Life Technologies) as previously described [26].

[1]H-magnetic resonance spectroscopy
^{1}H-MRS scans were performed at the CAMH Brain Health Imaging Centre (Toronto, Canada) using a 3T General Electric Discovery MR750 scanner (Milwaukee, WI, USA) equipped with an 8-channel head coil. Head motion was minimized by positioning each subject at the center of the head coil with soft restraint padding around the head and tape strapped across the forehead. All participants underwent T1-weighted (t1w) MRI scans (fast spoiled-gradient-echo 3-dimensional sagittal; FSPGR sequence, TE = 3.0 ms, TR = 6.7 ms, TI = 650 ms, flip angle = 8°, FOV = 28 cm, acquisition matrix 256 × 256 matrix, slice thickness = 0.9 mm).

Single voxel ^{1}H-MRS spectra were obtained using a standard GE Proton Brain Examination (PROBE) sequence with point-resolved spectroscopy (PRESS sequence, TE = 35 ms, TR = 2000 ms, number of excitations NEX = 8, bandwidth = 5000 Hz, 4096 data points used, 256 water-suppressed and 16 water-unsuppressed scans). Voxels ($10 \times 14 \times 30$ mm^3) were carefully positioned on the left hippocampus (Fig. 1). The signal over the voxel was shimmed to achieve a linewidth of 12 Hz or less, measured from the unsuppressed water peak in the voxel.

MRS data were analyzed with LCModel version 6.3-0E [43], using a standard basis set of metabolites at TE = 35 ms. The basis set contained L-alanine, aspartate, Cr, Cr methylene group, γ-aminobutyric acid, glucose, glutamate, glutamine, glutathione, glycerophosphocholine, L-lactate, mI, NAA, *N*-acetylaspartylglutamate, phosphocholine, phosphocreatine, scyllo-inositol, and taurine, as well as the following lipids (Lip) and macro-molecules (MM): Lip09, Lip13a, Lip13b, Lip20, MM09, MM12, MM14, MM17, and MM20.

Spectral fits yielded relative quantification of metabolite concentration levels. We then used the water-scaled metabolite results from LCmodel and corrected for fraction of water in each compartment (grey matter, white matter, and cerebrospinal fluid) as well as a relaxation term that accounts for the T1 and T2 of the water in each compartment (Supplementary Materials). Neurometabolite concentrations (including Glx) were thus expressed in institutional units (IU) that could be compared across individuals regardless of variations in the contribution of tissue composition to the voxel signal.

All scans included in statistical analyses met ^{1}H-MRS quality control cutoffs (full-width at half-maximum (FWHM) ≤0.1, signal-to-noise ratio (SNR) ≥10, Cramér-Rao lower bounds ≤20%), scans failing to meet QC cutoffs or meeting other criteria for rejecting analyses described in the LC Model manual [43] were removed from the analyses (detailed in Supplementary Materials).
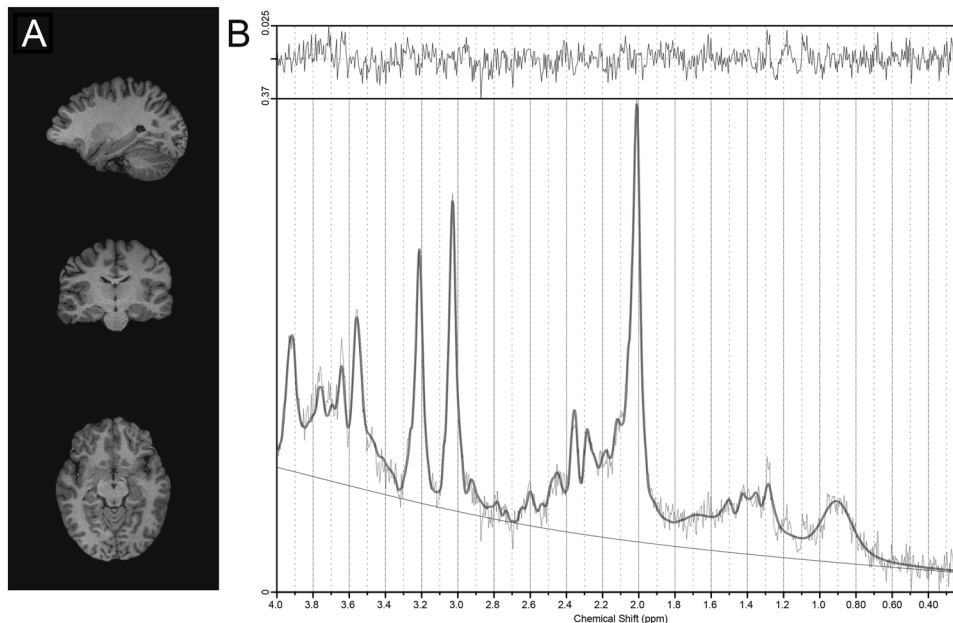
Fig. 1 Hippocampus voxel placement and ^{1}H-MRS spectrum. A Hippocampus voxel placement, and **B** ^{1}H-MRS spectrum (LC model output) for an individual participant included in the present analysis.

Hippocampus volume

MRI image pre-processing and total brain volume extraction. T1w MR images were converted to the MINC file format (https://www.mcgill.ca/bic/software/minc) and preprocessed using the minc-bpipe-library pre-processing pipeline from the CoBrA Laboratory tools (http://github.com/CobraLab/minc-bpipe-library). First, a two-step whole-scan bias field correction was applied using N4ITK [44]. Next, the image volume was cropped to remove excess data around the head to improve subsequent image processing steps. Finally, a brain mask computed using the BEaST patch based segmentation technique was used to calculate total intracranial volume (ICV; [45]).

Automatic segmentation of the hippocampus. Bilateral hippocampus volumes were extracted from pre-processed T1w images using MAGeT Brain, a multi-atlas segmentation algorithm [46, 47]. Briefly, five high-resolution atlases onto which structures have been manually segmented by anatomical experts [48] were used to label a set of 21 template scans, stratified across the data. Standard model-based segmentation procedure was performed using the ANTs algorithm for atlas-to-template nonlinear registration [44]. All subjects were then registered to the 21 templates, yielding 105 possible candidate segmentations; final segmentations were decided by a voxel-voting procedure [49]. Following segmentation, a quality control check was performed by visual inspection to ensure that labels respected anatomical borders. Scans that failed to meet quality control were removed from the analysis (Supplementary Materials).

Statistical analysis

Demographics were examined for group differences using independent-sample t-tests or chi-square tests. Sex was included as a covariate in light of the effect of sex on [^{11}C]CURB λk_3 [17] and on hippocampal glutamate [50]. Age was included as a covariate in all analysis as age differed between patient and control groups and has been associated with hippocampus Glx [51] and hippocampal volume [52]. Two participants from the healthy control group, and no participants from the psychosis group had the *FAAH* rs324420 AA genotype (Supplementary Tables S1 and S2). As the AA genotype is present only in one group, we have removed these participants from the primary analysis. Inclusion of the AA participants in the analysis did not have a meaningful impact on the outcomes of the primary analysis or the conclusions of this investigation (Supplementary Materials).

The present analysis includes a priori regions of interest consistent with those described in our study comparing FAAH between patients with psychotic disorders and healthy controls [17]; hippocampus, amygdala, limbic striatum, associative striatum, sensorimotor striatum, medial prefrontal cortex, anterior cingulate cortex and dorsolateral prefrontal cortex. The relationship between [^{11}C]CURB λk_3 and Glx was tested using a linear mixed effects model with [^{11}C]CURB λk_3 as the outcome measure, participant ID as a random effect (including intercept), region of interest as a repeated within-subject effect with a diagonal covariance structure, *FAAH* rs324420 (C385A) genotype, sex, and diagnostic group as fixed factors, and age as a covariate. For models testing hippocampal volume, total intracranial volume was also included as a covariate. Analyses including common sources of confounding as covariates (medications and tobacco use) are presented after reporting results without these variables. Effect sizes were calculated using sum of squares from SPSS version 25 and were interpreted as follows: Cohen's $f = 0.1$, small effect; Cohen's $f = 0.25$, medium effect; and Cohen's $f = 0.40$, a large effect [17]. All statistical tests were two-tailed, with $\alpha = 0.05$. For all analyses, interaction terms that were not significant were removed from the model. A significant main effect in the mixed-model — in the absence of a significant interaction with region of interest — indicates that the main effect is controlled for all regions studied.

RESULTS
Sample characteristics
Demographics and sample characteristics of the sample used in the FAAH and ^{1}H-MRS analysis are presented in table 1. Demographics and sample characteristics for the FAAH and hippocampal structure analysis are presented in supplementary table S1. For both analyses the psychosis group was older than the healthy control group. For the FAAH and ^{1}H-MRS analysis the psychosis group contained fewer female participants than the healthy control group. For the FAAH and hippocampus structure analysis only, the psychosis group had more smokers than the healthy control group. All participants tested negative for alcohol and drugs of abuse through urine toxicology. Although groups differed in total injected radioactivity (MBq), as expected MBq did not exert a significant effect on [^{11}C]CURB λk_3 ($F_{1,36.37} = 0.097$, $p = .76$; model controlled for all regions of interest, *FAAH* genotype, sex, and group) [53].

In line with results reported for overlapping samples [17, 35, 36], patients and healthy control participants did not differ with respect to [^{11}C]CURB λk_3 ($F_{1,36.41} = 1.04$, $p = 0.31$; controlling for 8 regions of interest, *FAAH* rs324420 genotype, and sex), Glx ($F_{1,33} = 0.00$, $p = 0.99$; controlling for age and sex), or

Table 1. Sample characteristics and clinical measures for [^{11}C]CURB and ^{1}H-MRS analysis (n or mean ± SD).

	Healthy control	Psychotic disorder	F/chi[a]	p
n	19	18		
Age (years)	21.7 ± 1.6	24.8 ± 6.0	4.84	0.034
BMI	24.5 ± 4.6	24.1 ± 5.0	0.31	0.58
Years of education	14.7 ± 1.7	15.0 ± 1.8	0.053	0.82
male/female	8/11	15/3	6.68	0.01
Handedness (right/left)	18/1	15/3	1.25	0.26
Tobacco non-smoker/smoker	19/0	16/2	—	0.23[b]
Medications & clinical profile				
Antidepressant	—	7		
Benzodiazepine	—	2		
Stimulant	—	2		
Antipsychotics (AP): AP-free/AP-treated/sub-therapeutic	—	11/3/4		
Mean antipsychotic dose (chlorpromazine-equivalent mg)[2]				
Therapeutic dose ($n = 3$)	—	521 ± 335		
Sub-therapeutic dose[c] ($n = 4$)	—	59 ± 20		
PANSS Total Score	—	58.2 ± 11.7		
Diagnosis (SZ/SF/SA/DD/NOS)	—	11/4/1/1/1		

BMI body mass index, AP antipsychotic, CPZ chlorpromazine, PANSS positive and negative syndrome scale, SZ schizophrenia, SF schizophreniform disorder, SA schizoaffective disorder, DD delusional disorder, NOS psychosis not otherwise specified.
[a]Mean dose for those taking antipsychotics; chlorpromazine equivalent doses calculated per Andreasen et al. 2010 [53].
[b]Fisher's exact test.
[c]Sub-therapeutic defined as doses below the equivalent starting dose of chlorpromazine (~200 mg/day).

hippocampus volume ($F_{1,40} = 0.63$, $p = 0.80$; controlling for age, sex, and total intracranial volume).

FAAH is associated with hippocampal Glx
Higher FAAH activity was associated with greater hippocampal Glx concentration (Fig. 2; $F_{1,36.36} = 9.17$, $p = 0.0045$; Cohen's $f = 0.30$, medium effect size, controlling for the eight regions sampled: hippocampus, amygdala, LST, AST, SMST, mPFC, ACC, DLPFC). This effect did not differ significantly by group ($F_{1,36.32} = 0.73$, $p = 0.40$) or brain region ($F_{1,55.57} = 1.82$, $p = 0.102$).

The relationship between FAAH activity and hippocampal Glx remained significant when controlling for antipsychotic use ($F_{1,36.39} = 9.45$, $p = 0.0040$) or antidepressant use ($F_{1,36.39} = 9.31$, $p = 0.0042$). Similarly, the effect remained significant if excluding smokers ($n = 2$; $F_{1,34.43} = 8.77$, $p = 0.0055$) or those taking benzodiazepines ($n = 2$; $F_{1,34.57} = 9.10$, $p = 0.0048$) or stimulants ($n = 2$; $F_{1,34.31} = 7.72$, $p = 0.0088$).

FAAH is associated with hippocampus structure
Higher FAAH activity was associated with smaller hippocampal volume (Fig. 3; $F_{1,44.70} = 5.94$, $p = 0.019$, Cohen's $f = 0.26$, medium effect size; controlling for the eight regions sampled). This effect did not differ significantly by group ($F_{1,44.73} = 2.73$, $p = 0.11$) or brain region ($F_{7,80.09} = 0.49$, $p = 0.84$). This effect remained significant when controlling for antipsychotic use ($F_{1,44.71} = 5.76$, $p = 0.021$) or antidepressant use ($F_{1,44.68} = 5.93$, $p = 0.019$). Similarly, the effect remained significant if excluding smokers ($n = 4$; $F_{1,40.71} = 5.73$, $p = 0.021$), those taking benzodiazepines ($n = 2$; $F_{1,42.77} = 6.71$, $p = 0.013$) or stimulants ($n = 3$; $F_{1,41.75} = 6.39$, $p = 0.015$).

DISCUSSION
Here we report that higher brain FAAH activity is associated with higher levels of hippocampal Glx and smaller hippocampal volume. Further, these effects did not differ significantly between young adults with and without psychotic disorders (no interaction). To our knowledge, links between brain FAAH activity, Glx, and brain structure have not previously been examined in vivo in humans.

The observation that higher FAAH activity was associated with higher Glx in the hippocampus is not without precedent. Preclinical data demonstrate that overexpression of FAAH in hippocampus led to elevated spontaneous glutamatergic and GABAergic neurotransmission [18]. Further support for links between the endocannabinoid and glutamate systems in the human brain comes from a report linking hippocampal cannabinoid CB1 receptors with Glx concentrations in the anterior cingulate cortex [54]. Future studies combining molecular neuroimaging with challenges to FAAH or glutamate may provide insight into a causative mechanism underlying these effects [55].

The finding that higher brain FAAH activity was associated with smaller hippocampal volume is supported by other studies in this field. The endocannabinoid system is involved in growth and development of the hippocampus through numerous mechanisms including interaction with neurotransmitters and neurotrophins [56, 57]. In older adults, lower hippocampal volume was associated with lower plasma levels of FAAH substrates [58]. In rodents, knockout of FAAH increased hippocampal progenitor cell proliferation [2] and elevating anandamide levels protected against stress-induced suppression of cell proliferation [31]. Further, increases of anandamide were implicated in exercise-induced increases in hippocampal cell proliferation [30]. Likewise, treatment with a FAAH inhibitor was associated with increased hippocampus BDNF and hippocampal cell proliferation in rodent models of depression or neuropathic pain [23–25]. These reports linking the endocannabinoid system with hippocampal cell proliferation in rodents support a potential link between the endocannabinoid system and hippocampal structure in humans [59].

There are several strengths to the design and methodology of the present study. Most patients were untreated, with only 3 patients in each analysis treated with antipsychotics at therapeutic
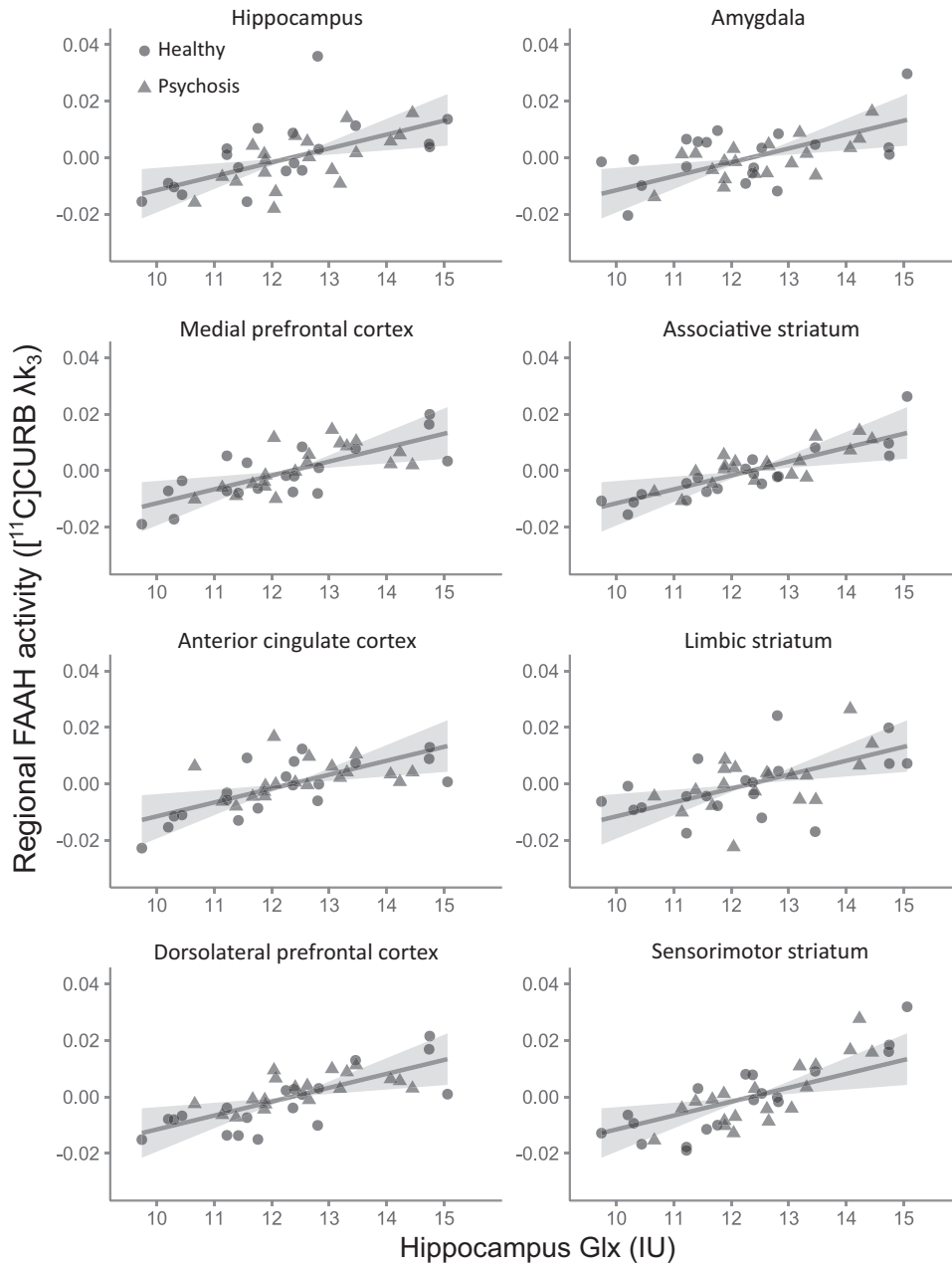
Fig. 2 Associations of hippocampus Glx with regional [^{11}C]CURB λk_3. Plots represent the random effects linear model fit ± 95% confidence intervals for the overall model fit. Scatter points represent partial residual values in each region for healthy volunteers (circles) and patients (triangles). Model controls for all regions, *FAAH* rs324420 genotype, age, sex, and diagnostic group. IU institutional units.

doses. Most patients were within 30 months of psychosis onset (mean: 20.7 ± 25.7 months; median 10 months) and had minimal exposure to antipsychotic medications, minimizing possible confounds related to past and ongoing exposure to antipsychotic medications.

Hippocampal FAAH activity was measured with the gold standard of PET methodology, using a metabolite-corrected arterial plasma input function and the validated [^{11}C]CURB λk_3, which has been demonstrated to be highly selective for FAAH [60] and is sensitive to changes in brain FAAH activity [26]. All participants completing [^{11}C]CURB PET scans were genotyped for the *FAAH* rs324420 polymorphism, known to affect FAAH protein levels [26]. Hippocampus ^{1}H-MRS conducted using a standard short-TE PRESS sequence was subjected to rigorous quality control and metabolite values were corrected for the T1 and T2 of water in

each tissue type contained within the voxel for each subject (Supplementary Materials).

The findings of this study should be interpreted in the context of several limitations. Using standard ^{1}H-MRS sequences at 3T it is difficult to reliably estimate glutamine due to spectral overlap with glutamate [61], therefore we utilized the composite outcome measure Glx, which has been reported to be elevated in psychosis-spectrum populations [62]. Studies at higher field strength or making use of acquisitions that have been optimized for estimating glutamine concentration could help to clarify whether FAAH activity is differently associated with glutamate or glutamine, or whether associations between FAAH activity and glutamine (rather than Glx) differ between patients and controls [62, 63].

Hippocampus volume as measured in the present study, did not differ significantly between groups (Supplementary Material).
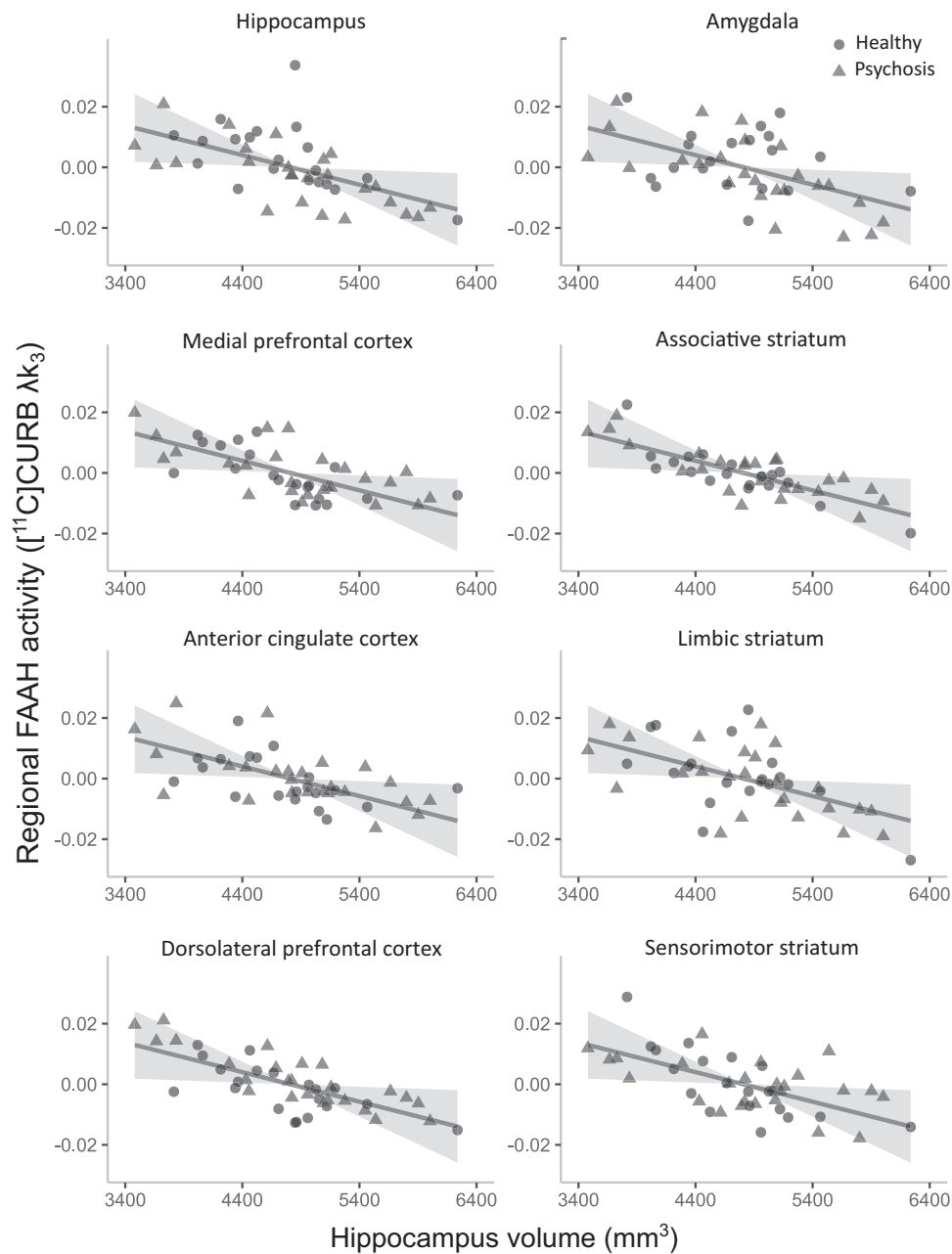
Fig. 3 Associations of hippocampus volume with regional [11C]CURB λk3. Plots represent the random effects linear model fit ±95% confidence intervals for the overall model fit. Scatter points represent partial residual values in each region for healthy volunteers (circles) and patients (triangles). Model controls for all regions, *FAAH* rs324420 genotype, age, sex, diagnostic group, and total intracranial volume.

Patients in the present study had first-episode psychosis, with most participants within 10 months of diagnosis. Although reduced hippocampus volume have been reported in first-episode and chronic schizophrenia [64], reduced hippocampus volume is associated with longer duration of untreated psychosis [65, 66]. Similarly, the finding of elevated hippocampus Glx is most robust in samples of patients with chronic schizophrenia [62], and has also been associated with longer duration of untreated psychosis (e.g., >12 months; 66). Characteristics of the sample in the present study – first-episode psychosis and short duration of untreated psychosis – may have contributed to the lack of group differences observed on both metrics. Therefore, a study of patients with chronic schizophrenia exhibiting elevated hippo-campus Glx and reduced hippocampus volume could provide greater insight into how FAAH may be related to altered hippocampus structure and glutamate in psychotic disorders [67, 68].

Individual differences in hippocampal volume could have affected the time-activity-curves (TACs) for [11C]CURB by the partial volume effect. However, it is expected that lower volume would produce reductions in the TAC and the λk3 – the opposite of what was observed in this analysis. Therefore, partial volume effects on [11C] CURB λk3 cannot explain the current findings.

Finally, the patient sample included only three female patients (five for hippocampal volume analysis). Preclinical studies have identified important contributions of sex to the functions of FAAH and anandamide in modulating hippocampal activity [20, 69]. Therefore, studies with larger numbers of female patients are necessary to determine whether the present findings generalize to female patients with psychotic disorders.

Taken together, results from this study provide evidence that links between the endocannabinoid system and hippocampus neurotransmission and structure that have been previously observed in animals, are conserved in humans.

By combining [^{11}C]CURB PET, ^{1}H-MRS and structural MRI, the present study provides the first in vivo evidence in humans linking the brain endocannabinoid system with hippocampal glutamate metabolites and hippocampal volume. Across brain regions, higher FAAH activity was associated with higher glutamate metabolite concentrations and smaller hippocampal volumes in young adults.

REFERENCES

1. Lieberman J, Girgis R, Brucato G, Moore H, Provenzano F, Kegeles L, et al. Hippocampal dysfunction in the pathophysiology of schizophrenia: a selective review and hypothesis for early detection and intervention. Mol Psychiatry. 2018;23:1764–72.
2. Aguado T, Monory K, Palazuelos J, Stella N, Cravatt B, Lutz B, et al. The endocannabinoid system drives neural progenitor proliferation. FASEB J. 2005;19:1704–6. https://doi.org/10.1096/fj.05-3995fje.
3. Berghuis P, Dobszay MB, Wang X, Spano S, Ledda F, Sousa KM, et al. Endocannabinoids regulate interneuron migration and morphogenesis by transactivating the TrkB receptor. Proc Natl Acad Sci. 2005;102:19115–20.
4. Harkany T, Guzmán M, Galve-Roperh I, Berghuis P, Devi LA, Mackie K. The emerging functions of endocannabinoid signaling during CNS development. Trends Pharmacol Sci. 2007;28:83–92. https://doi.org/10.1016/j.tips.2006.12.004
5. Gao Y, Vasilyev DV, Goncalves MB, Howell FV, Hobbs C, Reisenberg M, et al. Loss of retrograde endocannabinoid signaling and reduced adult neurogenesis in diacylglycerol lipase knock-out mice. J Neurosci. 2010;30:2017–24.
6. Jenniches I, Ternes S, Albayram O, Otte DM, Bach K, Bindila L, et al. Anxiety, Stress, and Fear Response in Mice With Reduced Endocannabinoid Levels. Biol Psychiatry. 2016;79:858–68. https://doi.org/10.1016/j.biopsych.2015.03.033.
7. Katona I, Freund TF. Endocannabinoid signaling as a synaptic circuit breaker in neurological disease. Nat Med. 2008;14:923–30.
8. Curran HV, Freeman TP, Mokrysz C, Lewis DA, Morgan CJA, Parsons LH. Keep off the grass? Cannabis, cognition and addiction. Nat Rev Neurosci. 2016;17:293–306. https://doi.org/10.1038/nrn.2016.28.
9. Galve-Roperh I, Aguado T, Palazuelos J, Guzmán M. Mechanisms of control of neuron survival by the endocannabinoid system. Curr Pharm Des. 2008;14:2279–88.
10. Kano M, Ohno-Shosaku T, Hashimotodani Y, Uchigashima M, Watanabe M. Endocannabinoid-mediated control of synaptic transmission. Physiol. Rev. 2009; 309–80.
11. Chávez AE, Chiu CQ, Castillo PE. TRPV1 activation by endogenous anandamide triggers postsynaptic long-term depression in dentate gyrus. Nat Neurosci. 2010;13:1511.
12. Di Marzo V. Anandamide serves two masters in the brain. Nat Neurosci. 2010;13:1446–8.
13. Minichino A, Senior M, Brondino N, Zhang SH, Godwleska BR, Burnet PW, et al. Measuring disturbance of the endocannabinoid system in psychosis: a systematic review and meta-analysis. JAMA Psychiatry. 2019;76:914–23.
14. Garani R, Watts JJ, Mizrahi R. Endocannabinoid system in psychotic and mood disorders, a review of human studies. Prog Neuropsychopharmacol Biol Psychiatry. 2021;106:110096. https://doi.org/10.1016/j.pnpbp.2020.110096.
15. Muguruza C, Lehtonen M, Aaltonen N, Morentin B, Meana JJ, Callado LF. Quantification of endocannabinoids in postmortem brain of schizophrenic subjects. Schizophr Res. 2013;148:145–50. https://doi.org/10.1016/j.schres.2013.06.013.
16. Cravatt BF, Demarest K, Patricelli MP, Bracey MH, Giang DK, Martin BR, et al. Supersensitivity to anandamide and enhanced endogenous cannabinoid signaling in mice lacking fatty acid amide hydrolase. Proc Natl Acad Sci USA 2001;98:9371–6. https://doi.org/10.1073/pnas.161191698.
17. Watts JJ, Jacobson MR, Lalang N, Boileau I, Tyndale RF, Kiang M, et al. Imaging brain fatty acid amide hydrolase in untreated patients with psychosis. Biol Psychiatry. 2020;88:727–35. https://doi.org/10.1016/j.biopsych.2020.03.003.
18. Zimmermann T, Bartsch JC, Beer A, Lomazzo E, Guggenhuber S, Lange MD, et al. Impaired anandamide/palmitoylethanolamide signaling in hippocampal glutamatergic neurons alters synaptic plasticity, learning, and emotional responses. Neuropsychopharmacology. 2019;44:1377–88. https://doi.org/10.1038/s41386-018-0274-7.
19. Hakimizadeh E, Oryan S. Endocannabinoid system and TRPV1 receptors in the dorsal hippocampus of the rats modulate anxiety-like behaviors. Iran J basic Med Sci. 2012;15:795.
20. Huang GZ, Woolley CS. Estradiol acutely suppresses inhibition in the hippocampus through a sex-specific endocannabinoid and mGluR-dependent mechanism. Neuron. 2012;74:801–8.
21. Wang M, Hill MN, Zhang L, Gorzalka BB, Hillard CJ, Alger BE. Acute restraint stress enhances hippocampal endocannabinoid function via glucocorticoid receptor activation. J Psychopharmacol. 2012;26:56–70.
22. Aguilar DD, Giuffrida A, Lodge DJ. THC and endocannabinoids differentially regulate neuronal activity in the prefrontal cortex and hippocampus in the subchronic PCP model of schizophrenia. J Psychopharmacol. 2015;30:169–81. https://doi.org/10.1177/0269881115612239.
23. Jiang HX, Liu J, Ma G, Hai K-r, Gong D-y, Ke BW. et al. Inhibition of fatty acid amide hydrolase improves depressive-like behaviors independent of its peripheral antinociceptive effects in a rat model of neuropathic pain. Anesthesia Analgesia. 2019;129:587–97. https://doi.org/10.1213/ane.0000000000003563.
24. Carnevali L, Statello R, Vacondio F, Ferlenghi F, Spadoni G, Rivara S, et al. Antidepressant-like effects of pharmacological inhibition of FAAH activity in socially isolated female rats. Eur Neuropsychopharmacol. 2020;32:77–87. https://doi.org/10.1016/j.euroneuro.2019.12.119.
25. Tejeda-Martínez AR, Viveros-Paredes JM, Hidalgo-Franco GV, Pardo-González E, Chaparro-Huerta V, González-Castañeda RE, et al. Chronic inhibition of FAAH reduces depressive-like behavior and improves dentate gyrus proliferation after chronic unpredictable stress exposure. Behavioural Neurol. 2021;2021:6651492 https://doi.org/10.1155/2021/6651492.
26. Boileau I, Tyndale RF, Williams B, Mansouri E, Westwood DJ, Le Foll B, et al. The fatty acid amide hydrolase C385A variant affects brain binding of the positron emission tomography tracer [(11)C]CURB. J Cereb Blood Flow Metab. 2015;35:1237–40. https://doi.org/10.1038/jcbfm.2015.119.
27. Gee DG, Fetcho RN, Jing D, Li A, Glatt CE, Drysdale AT, et al. Individual differences in frontolimbic circuitry and anxiety emerge with adolescent changes in endocannabinoid signaling across species. Proc Natl Acad Sci. 2016;113:4500–5. https://doi.org/10.1073/pnas.1600013113.
28. Dincheva I, Drysdale AT, Hartley CA, Johnson DC, Jing D, King EC, et al. FAAH genetic variation enhances fronto-amygdala function in mouse and human. Nat Commun. 2015;6:6395 https://doi.org/10.1038/ncomms7395.
29. Zabik NL, Iadipaolo AS, Marusak HA, Peters C, Burghardt K, Rabinak CA. A common genetic variant in fatty acid amide hydrolase is linked to alterations in fear extinction neural circuitry in a racially diverse, nonclinical sample of adults. J Neurosci Res. 2021. https://doi.org/10.1002/jnr.24860.
30. Hill MN, Titterness AK, Morrish AC, Carrier EJ, Lee TTY, Gil-Mohapel J, et al. Endogenous cannabinoid signaling is required for voluntary exercise-induced enhancement of progenitor cell proliferation in the hippocampus. Hippocampus. 2010;20:513–23.
31. Hill MN, Kambo JS, Sun JC, Gorzalka BB, Galea LAM. Endocannabinoids modulate stress-induced suppression of hippocampal cell proliferation and activation of defensive behaviours. Eur J Neurosci. 2006;24:1845–9. https://doi.org/10.1111/j.1460-9568.2006.05061.x.
32. Kraguljac NV, White DM, Reid MA, Lahti AC. Increased hippocampal glutamate and volumetric deficits in unmedicated patients with schizophrenia. JAMA Psychiatry. 2013;70:1294–302.
33. Bogerts B, Lieberman JA, Ashtari M, Bilder RM, Degreef G, Lerner G, et al. Hippocampus-amygdala volumes and psychopathology in chronic schizophrenia. Biol Psychiatry. 1993;33:236–46. https://doi.org/10.1016/0006-3223(93)90289-p.
34. Kay SR, Fiszbein A, Opler LA. The positive and negative syndrome scale (PANSS) for schizophrenia. Schizophrenia Bull. 1987;13:261–76.
35. Shakory S, Watts JJ, Hafizi S, Da Silva T, Khan S, Kiang M, et al. Hippocampal glutamate metabolites and glial activation in clinical high risk and first episode psychosis. Neuropsychopharmacology. 2018;43:2249–55.
36. Hafizi S, Guma E, Koppel A, Da Silva T, Kiang M, Houle S, et al. TSPO expression and brain structure in the psychosis spectrum. Brain Behav Immun. 2018;74:79–85.
37. Appelbaum PS, Grisso T. MacArthur competence assessment tool for clinical research (MacCAT-CR): professional resource press/professional resource exchange. 2001.
38. Rusjan PM, Wilson AA, Mizrahi R, Boileau I, Chavez SE, Lobaugh NJ, et al. Mapping human brain fatty acid amide hydrolase activity with PET. J Cereb Blood Flow Metab. 2013;33:407–14. doi:jcbfm2012180 [pii] 10.1038/jcbfm.2012.180.
39. Alexander JP, Cravatt BF. Mechanism of carbamate inactivation of FAAH: implications for the design of covalent inhibitors and in vivo functional probes for enzymes. Chem Biol. 2005;12:1179–87.
40. Mileni M, Kamtekar S, Wood DC, Benson TE, Cravatt BF, Stevens RC. Crystal structure of fatty acid amide hydrolase bound to the carbamate inhibitor URB597: discovery of a deacylating water molecule and insight into enzyme inactivation. J Mol Biol. 2010;400:743–54.
41. Wilson AA, Garcia A, Parkes J, Houle S, Tong J, Vasdev N. [11C]CURB: Evaluation of a novel radiotracer for imaging fatty acid amide hydrolase by positron emission

tomography. Nucl Med Biol. 2011;38:247–53. https://doi.org/10.1016/j.nucmedbio.2010.08.001.

42. Rusjan P, Mamo D, Ginovart N, Hussey D, Vitcu I, Yasuno F, et al. An automated method for the extraction of regional data from PET images. Psychiatry Res Neuroimaging. 2006;147:79–89.

43. Provencher SW. LCModel & LCMgui user's manual. LCModel Version. 2014;6:2–3.

44. Avants BB, Tustison NJ, Song G, Cook PA, Klein A, Gee JC. A reproducible evaluation of ANTs similarity metric performance in brain image registration. Neuroimage. 2011;54:2033–44.

45. Eskildsen SF, Coupé P, Fonov V, Manjón JV, Leung KK, Guizard N, et al. BEaST: brain extraction based on nonlocal segmentation technique. NeuroImage. 2012;59:2362–73.

46. Chakravarty MM, Steadman P, van Eede MC, Calcott RD, Gu V, Shaw P, et al. Performing label-fusion-based segmentation using multiple automatically generated templates. Hum Brain Mapp. 2013;34:2635–54.

47. Pipitone J, Park MTM, Winterburn J, Lett TA, Lerch JP, Pruessner JC, et al. Multi-atlas segmentation of the whole hippocampus and subfields using multiple automatically generated templates. Neuroimage. 2014;101:494–512.

48. Winterburn JL, Pruessner JC, Chavez S, Schira MM, Lobaugh NJ, Voineskos AN, et al. A novel in vivo atlas of human hippocampal subfields using high-resolution 3 T magnetic resonance imaging. Neuroimage. 2013;74:254–65.

49. Collins DL, Pruessner JC. Towards accurate, automatic segmentation of the hippocampus and amygdala from MRI by augmenting ANIMAL with a template library and label fusion. Neuroimage. 2010;52:1355–66. https://doi.org/10.1016/j.neuroimage.2010.04.193.

50. Hädel S, Wirth C, Rapp M, Gallinat J, Schubert F. Effects of age and sex on the concentrations of glutamate and glutamine in the human brain. J Magn Reson Imaging. 2013;38:1480–7.

51. Roalf DR, Sydnor VJ, Woods M, Wolk DA, Scott JC, Reddy R, et al. A quantitative meta-analysis of brain glutamate metabolites in aging. Neurobiol Aging. 2020;95:240–9. https://doi.org/10.1016/j.neurobiolaging.2020.07.015.

52. Walhovd KB, Westlye LT, Amlien I, Espeseth T, Reinvang I, Raz N, et al. Consistent neuroanatomical age-related volume differences across multiple samples. Neurobiol Aging. 2011;32:916–32. https://doi.org/10.1016/j.neurobiolaging.2009.05.013.

53. Andreasen NC, Pressler M, Nopoulos P, Miller D, Ho BC. Antipsychotic dose equivalents and dose-years: a standardized method for comparing exposure to different drugs. Biol Psychiatry. 2010;67:255–62. https://doi.org/10.1016/j.biopsych.2009.08.040.

54. Borgan F, Veronese M, Reis Marques T, Lythgoe DJ, Howes O. Association between cannabinoid 1 receptor availability and glutamate levels in healthy controls and drug-free patients with first episode psychosis: a multi-modal PET and 1H-MRS study. Eur Archives Psychiatry Clin Neurosci. 2020. https://doi.org/10.1007/s00406-020-01191-2.

55. Kraguljac NV, Frolich MA, Tran S, White DM, Nichols N, Barton-McArdle A, et al. Ketamine modulates hippocampal neurochemistry and functional connectivity: a combined magnetic resonance spectroscopy and resting-state fMRI study in healthy volunteers. Mol Psychiatry. 2017;22:562–9. https://doi.org/10.1038/mp.2016.122.

56. Rizos E, Papathanasiou M, Michalopoulou P, Mazioti A, Douzenis A, Kastania A, et al. Association of serum BDNF levels with hippocampal volumes in first psychotic episode drug-naive schizophrenic patients. Schizophr Res. 2011;129:201–4.

57. Bambico FR, Gobbi G. The cannabinoid CB1 receptor and the endocannabinoid anandamide: possible antidepressant targets. Expert Opin Ther Targets. 2008;12:1347–66. https://doi.org/10.1517/14728222.12.11.1347.

58. Kim M, Snowden S, Suvitaival T, Ali A, Merkler DJ, Ahmad T, et al. Primary fatty amides in plasma associated with brain amyloid burden, hippocampal volume, and memory in the European Medical Information Framework for Alzheimer's Disease biomarker discovery cohort. Alzheimer's Dement. 2019;15:817–27. https://doi.org/10.1016/j.jalz.2019.03.004.

59. Heyman E, Gamelin F-X, Goekint M, Piscitelli F, Roelands B, Leclair E, et al. Intense exercise increases circulating endocannabinoid and BDNF levels in humans—possible implications for reward and depression. Psychoneuroendocrinology. 2012;37:844–51.

60. Boileau I, Rusjan PM, Williams B, Mansouri E, Mizrahi R, De Luca V, et al. Blocking of fatty acid amide hydrolase activity with PF-04457845 in human brain: a positron emission tomography study with the novel radioligand [C]CURB. J Cereb Blood Flow Metab. 2015. https://doi.org/10.1038/jcbfm.2015.133.

61. Snyder J, Wilman A. Field strength dependence of PRESS timings for simultaneous detection of glutamate and glutamine from 1.5 to 7T. J Magn Reson. 2010;203:66–72. https://doi.org/10.1016/j.jmr.2009.12.002.

6-

2.

62. Merritt K, Egerton A, Kempton MJ, Taylor MJ, McGuire PK. Nature of glutamate alterations in schizophrenia: a meta-analysis of proton magnetic resonance spectroscopy studies. JAMA Psychiatry. 2016;73:665–74.

63. Agarwal N, Renshaw P. Proton MR spectroscopy–detectable major neurotransmitters of the brain: Biology and possible clinical applications. Am J Neuroradiol. 2012;33:595–602.

64. Adriano F, Caltagirone C, Spalletta G. Hippocampal volume reduction in first-episode and chronic schizophrenia: a review and meta-analysis. Neuroscientist. 2012;18:180–200.

65. Goff DC, Zeng B, Ardekani BA, Diminich ED, Tang Y, Fan X, et al. Association of hippocampal atrophy with duration of untreated psychosis and molecular biomarkers during initial antipsychotic treatment of first-episode psychosis. JAMA Psychiatry. 2018;75:370–8.

66. Briend F, Nelson EA, Maximo O, Armstrong WP, Kraguljac NV, Lahti AC. Hippocampal glutamate and hippocampus subfield volumes in antipsychotic-naive first episode psychosis subjects and relationships to duration of untreated psychosis. Transl Psychiatry. 2020;10:1–11.

67. McHugo M, Talati P, Woodward ND, Armstrong K, Blackford JU, Heckers S. Regionally specific volume deficits along the hippocampal long axis in early and chronic psychosis. NeuroImage Clin. 2018;20:1106–14. https://doi.org/10.1016/j.nicl.2018.10.021.

68. Wannan CM, Cropley VL, Chakravarty MM, Van Rheenen TE, Mancuso S, Bousman C, et al. Hippocampal subfields and visuospatial associative memory across stages of schizophrenia-spectrum disorder. Psychological Med. 2019;49:2452–62.

69. Tabatadze N, Huang G, May RM, Jain A, Woolley CS. Sex differences in molecular signaling at inhibitory synapses in the Hippocampus. J Neurosci. 2015;35:11252–65. https://doi.org/10.1523/jneurosci.1067-15.2015.

AUTHOR CONTRIBUTIONS
RM designed the study. JJW performed the analyses supervised by RM. RM confirmed DSM-IV diagnostic status. JJW analyzed PET images, advised by PMR. JJW analyzed ^{1}H-MRS, advised by SC. JJW drafted the manuscript with input from RM. EG managed structural MRI processing and quantification of hippocampal and intracranial volumes, advised by MC. RFT managed FAAH genotyping. RAR consulted on the endocannabinoid system. AAW designed and advised on [^{11}C]CURB. RM, SH provided medical coverage for [^{11}C]CURB PET scans. All authors provided critical feedback on the manuscript.

COMPETING INTERESTS
RM is part of the SAB for a particular program at BI. RFT has consulted for Apotex and Quinn Emanuel, and Ethismos on unrelated topics. All other authors declare no competing interests.

ADDITIONAL INFORMATION
Supplementary information The online version contains supplementary material available at https://doi.org/10.1038/s41386-022-01384-4.

Correspondence and requests for materials should be addressed to Romina Mizrahi.

Reprints and permission information is available at http://www.nature.com/reprints

Publisher's note Springer Nature remains neutral with regard to jurisdictional claims in published maps and institutional affiliations.